Interface magnetization effect in heterojunctions based on semimagnetic compounds

N. Malkova*
Institute of Applied Physics, AS of Moldova, 2028 Kishinev, Moldova
and The Abdus Salam International Centre for Theoretical Physics, Trieste, Italy
(Received 18 August 1998)

The electronic states of stressed heterojunctions formed from narrow-gap semimagnetic semiconductors showing antiferromagnetic ordering are studied. The model Hamiltonian is constructed in the framework of the two-band envelope-function approximation including far-band corrections. Heterojunctions, both with normal and inverted band arrangements in the initial semiconductors, are investigated. The interface Tamm-like states have been shown recently to appear in these heterojunctions, and they are spin split with the magnetic axis perpendicular to the interface plane. The effect of far-band corrections is shown to be conditioned by the mutual movement of the constituent bands, resulting in changes and in some cases in the full disappearance of the energy interval in which the interface state exists. The interface magnetization effect is expected when the Fermi level lies in one of the spin-polarized interface bands. Using the appropriate parameters, the value of the relative interface magnetization is calculated. [S0163-1829(99)03403-7]

I. INTRODUCTION

Dilute magnetic (semimagnetic) semiconductors are formed by replacing a fraction of the cations in a host semiconductor alloy with transition-metal ions. The presence of a magnetic component introduces specific properties related to the strong coupling of the spins of the band electrons or holes of a semiconductor to localized magnetic moments due to the *d* or *f* electrons of the transition metals. Quantum structures based on semimagnetic narrow-gap IV-VI or II-VI semiconductors are currently of great interest because of their interesting physical properties and technological importance. It is now recognized that interfaces play the most important role in magnetic properties. The key to understanding the interface magnetization effects lies in the structure of the interface plane, its imperfection, and the disposition of the magnetic impurities across the interface,[1] and in the electronic structure, especially the existence of the spin-polarized surface states.[2,3] A theoretical model of the interface magnetization effect starting from the magnetic properties of the Tamm's interface states, arising in some narrow-gap stressed semimagnetic heterojunctions with antiferromagnetic ordering, was developed in previous papers.[4,5] As model materials, the heterojunctions based on semimagnetic narrow-gap IV-VI semiconductors with mutually inverted bands (that is, the constituent gaps are opposite in sign) were considered. Interface spin-split states were shown to appear in these structures. It is a semimagnetic constituent which is responsible for antiferromagnetic ordering, which conditions the nonzero average spin value bound to each interface state. If the Fermi level lies in one of the interface bands, magnetic ordering appears in the interface plane. In this context the interface magnetization effect was discussed in Refs. 4 and 5. It is important to note that the existence of the spin-polarized states, present in antiferromagnetic coupled systems, was also derived in Refs. 2 and 3 using a simple model of a semi-infinite linear chain of atoms with one spin orbital per site which was treated within the tight-binding framework.

The simplest theoretical model for the narrow-gap IV-VI semiconductors is a two-band one. In the first approximation of the $\mathbf{k}\cdot\hat{\mathbf{p}}$ perturbation theory, including only matrix elements between near-band states, this model reduces to the Dirac Hamiltonian. This approach was effectively used in Refs. 4–6, after the first investigations in Refs. 7 and 8. This approximation yields an analytical solution, giving an opportunity to observe the genesis of the interface states, and in this way to understand their nature. However, this approach was shown to be justified only at energies small compared to the gap energy. In the next approximation, the effects of more distant bands are well known to be treated in the second-order perturbation theory. These effects proved to be of most importance for heterojunctions with a normal band arrangement (that is, with $E_{ga}E_{gb}>0$). We call these structures normal, in contrast to the inverted structures with mutually inverted bands. It has been shown that the same interface states appear in the normal heterojunctions.[6,8] If, in the inverted contact, the states are located in the gap of the constituent semiconductors, and there is a real energy region in which the lowest order $\mathbf{k}\cdot\hat{\mathbf{p}}$-perturbation theory is satisfied, then in the normal heterojunction the situation is more complicated. In this case the interface states were shown to be usually located inside either the conduction or valence bands of the constituents.[6,8] Then the far-band corrections have to be included in the Hamiltonian.

In this paper we discuss the effects of far-band corrections on the interface states. However, in order to observe the change of the energy spectrum with the increasing sophistication of the model, and so as not to complicate the analysis, we retain the other approximations used in Refs. 4 and 5. Thus the aim of this work is to study the interface states in stressed heterojunctions, both with the normal and inverted band arrangements, based on narrow-gap semiconductors showing antiferromagnetic ordering, taking into account far-band corrections. Although our results are more generally applicable, we use heterojunctions based on semimagnetic narrow-gap IV-VI semiconductors as model materials.

The paper is organized as follows. In Sec. II we briefly

describe the theoretical model. In Sec. III we derive analytical results for the bulk and interface electronic states for some special limiting cases. In Sec. IV a perturbation solution, as well as corresponding numerical results for the interface states, are presented. Interface magnetization is studied in Sec. V. This is followed by a brief summary at the end.

II. MODEL HAMILTONIAN

The electronic properties of heterostructures composed of semiconductors which have a similar band structure can be described by an envelope-function formalism reduced to a $\mathbf{k}\cdot\hat{\mathbf{p}}$-band model with spatially varying material parameters.[9] The constituents of the heterojunctions are narrow-gap materials ($E_g<0.5$ eV) with the two nearest bands forming a direct band gap at L points of the Brillouin zone. The far bands are remote by energies large compared to the gap energy. It is usually sufficient to take into account coupling between the doubly degenerate conduction and valence bands exactly, while treating the far bands in perturbation up to order k^2.[10] Within the mirror symmetry band approximation, assuming the axis z to be parallel to the trigonal [111] crystal axis, one obtains a Hamiltonian for the heterostructure with the axis along the same z direction in the form

$$\hat{H}_{00}=\begin{pmatrix} \Delta(z)+V(z)+\dfrac{\hbar^2k_\perp^2}{2m_\perp}-\dfrac{\hbar^2}{2m_\parallel}\dfrac{\partial^2}{\partial z^2} & \boldsymbol{\sigma}\cdot\mathbf{p} \\ \boldsymbol{\sigma}\cdot\hat{\mathbf{p}} & -\Delta(z)+V(z)-\dfrac{\hbar^2k_\perp^2}{2m_\perp}+\dfrac{\hbar^2}{2m_\parallel}\dfrac{\partial^2}{\partial z^2} \end{pmatrix}. \tag{1}$$

Here $\Delta(z)=E_g(z)/2$, $V(z)$ is a so-called work function describing the shift of the constituent gap middles, the momentum operator $\hat{\mathbf{p}}$ for the structures under consideration is reduced to $\hat{\mathbf{p}}=-i\hbar(v_\perp k_x, v_\perp k_y, v_\parallel\nabla_z)$ (where k_x and k_y are the components of the transverse momentum vector with the length $k_\perp$, and $v_\perp$ and $v_\parallel$ are the interband matrix elements of the velocity operator), and $\boldsymbol{\sigma}=(\sigma_x,\sigma_y,\sigma_z)$ is the vector with the components of the Pauli matrices $\sigma_{x,y,z}$. Finally, $m_\perp$ and $m_\parallel$ are the far-band contributions to the effective masses which are taken equal to the same value for the conduction and valence bands within the mirror symmetry band model. The dependence of the far-band masses on the coordinate z (far-band mass mismatch) is neglected here, and so the multiplier $1/m_\parallel$ was taken out of the differential in the operator $(\partial/\partial z)(1/m_\parallel)(\partial/\partial z)$ of the diagonal Hamiltonian components.

Two more terms need to be included in the Hamiltonian. The first describes the polarization effect induced by the strain,[4]

$$\hat{H}_{\rm st}=\begin{pmatrix} 0 & -i\boldsymbol{\sigma}\mathbf{E} \\ i\boldsymbol{\sigma}\mathbf{E} & 0 \end{pmatrix}, \tag{2}$$

where the vector $\mathbf{E}$ is determined by the mutual shifts of the cation and anion sublattices of the initial semiconductors along three directions. Taking into account the results of experimental work,[11] we presume the polarization to be $\mathbf{E}=(0,0,E)$.

The second term describes the exchange interaction between the magnetic impurity spin and electron spins. Assuming the magnetic impurities to be localized at the interstitials, with the spins antiferromagnetically arranged along the z axis, we obtain[4]

$$\hat{H}_{\rm ex}=\begin{pmatrix} 0 & -iL \\ iL & 0 \end{pmatrix}, \tag{3}$$

where L is the matrix element of the exchange interaction constructed on wave functions with the symmetry of the actual bands. Both $\hat{H}_{\rm st}$ and $\hat{H}_{\rm ex}$ have been discussed in previous work,[4] where some numerical values of E and L were given.

Thus our model Hamiltonian for the stressed IV-VI semiconductor heterojunction showing the antiferromagnetic ordering along the z axis reads

$$\hat{H}=\hat{H}_{00}+\hat{H}_{\rm st}+\hat{H}_{\rm ex}. \tag{4}$$

We see that $\hat{H}$ commutes with $\hat{W}=\boldsymbol{\sigma}[\hat{\mathbf{p}}\cdot\mathbf{n}]+\sigma_z L$ (where $\mathbf{n}$ is the unit vector along the axis z). Hence, making use of the eigenfunctions $\hat{W}$ as a basis, we can reduce the Schrödinger equation to

$$\begin{pmatrix} \Delta-V+\dfrac{\hbar^2k_\perp^2}{2m_\perp}-\dfrac{\hbar^2}{2m_\parallel}\dfrac{\partial^2}{\partial z^2}-\epsilon & \hbar v_\parallel\dfrac{\partial}{\partial z}+W_\pm+E \\ -\hbar v_\parallel\dfrac{\partial}{\partial z}+W_\pm+E & -\Delta-V-\dfrac{\hbar^2k_\perp^2}{2m_\perp}+\dfrac{\hbar^2}{2m_\parallel}\dfrac{\partial^2}{\partial z^2}-\epsilon \end{pmatrix}\begin{pmatrix}\varphi^\pm\\ \chi^\pm\end{pmatrix}=0. \tag{5}$$

Here $W_{\pm}$, and $\varphi^{\pm}$ and $\chi^{\pm}$, are the eigenvalues and eigenfunctions of the operator $\hat{W}$ determined by the relations $W_{\pm}=\pm\hbar v_{\perp}\sqrt{\tilde{L}^2+k_{\perp}^2}$ and

$$\varphi^{\pm}(\chi^{\pm})=\varphi_0^{\pm}(\chi_0^{\pm})\begin{pmatrix}1\\ \dfrac{k_y-ik_x}{\tilde{L}+W_{\pm}}\end{pmatrix}, \tag{6}$$

where $\varphi_0^{\pm}$ and $\chi_0^{\pm}$ are normalized factors, and $\tilde{L}=L/\hbar v_{\perp}$.

We begin the study of Eq. (5) by choosing values of Δ and E equal to some constants, and setting $V=0$. Then the energy spectrum of the homogeneous semiconductor with polarization and antiferromagnetic ordering is found to be

$$\epsilon_{\pm}^{c}=\left[(E+W_{\pm})^2+\left(\Delta+\frac{\hbar^2k_{\perp}^2}{2m_{\perp}}+\frac{\hbar^2k_{\parallel}^2}{2m_{\parallel}}\right)^2+\hbar^2v_{\parallel}^2k_{\parallel}^2\right]^{1/2},$$

$$\epsilon_{\pm}^{v}=-\left[(E+W_{\pm})^2+\left(\Delta+\frac{\hbar^2k_{\perp}^2}{2m_{\perp}}+\frac{\hbar^2k_{\parallel}^2}{2m_{\parallel}}\right)^2+\hbar^2v_{\parallel}^2k_{\parallel}^2\right]^{1/2}, \tag{7}$$

where $k_{\parallel}$ is the component of the momentum along the trigonal axis, and the indices c and v indicate the branches related to the conduction and valence bands, respectively. The polarization and antiferromagnetic ordering have been shown to split the Kramers spin degeneracy.[4] As a result, each of the branches of the conduction $\epsilon_{\pm}^{c}$ or valence $\epsilon_{\pm}^{v}$ bands is characterized by opposite directions of the spin, with the average spin vector being

$$\vec{S}^{\pm}=\pm\frac{1}{\sqrt{\tilde{L}^2+k_{\perp}^2}}(k_y,-k_x,0), \tag{8}$$

where the sign ''+'' is related to branches with the index ''+'', and the sign ''−'' to branches with the index ''−''.

If a heterostructure with the axis along z is considered, the parameters Δ, E, and V are functions depending on the coordinate z. The Schrödinger equation (5) is a set of two second-order differential equations. There is no way of solving this eigenvalue problem analytically in the general case. By applying proper boundary conditions one can obtain a numerical solution. Before doing so, it is useful to consider some special cases having analytical solutions.

III. SIMPLE HETEROCONTACT

Considering the ''simple'' heterocontact implies that in the Schrödinger equation (5) one should put $L=0$ and $E=0$. This case was discussed in Ref. 8. However, we are interested in the same problem from another point of view.

When $L=E=0$ the transformation of the wave functions into the form $u^{\pm}=\varphi^{\pm}+\chi^{\pm}$, $v^{\pm}=\varphi^{\pm}-\chi^{\pm}$ reduces the eigenvalue equation (5) to

$$\begin{pmatrix}\mp\hbar v_{\perp}k_{\perp}+V-\epsilon & \left(\Delta(z)+\dfrac{\hbar^2k_{\perp}^2}{2m_{\perp}}-\dfrac{\hbar^2}{2m_{\parallel}}\dfrac{\partial^2}{\partial z^2}\right)+ip_z\\ \text{H.c.} & \pm\hbar v_{\perp}k_{\perp}+V-\epsilon\end{pmatrix}\begin{pmatrix}u^{\pm}\\ v^{\pm}\end{pmatrix}=0. \tag{9}$$

If the gap centers of the constituents are aligned throughout, so that $V(z)=V$ is a constant, then there exists a solution with $u^{\pm}=0$ or $v^{\pm}=0$, depending on the drift of the $\Delta(z)$ function. For example, in the case $\Delta(+\infty)>\Delta(-\infty)$, Eq. (9) admits a solution with $u^{\pm}=0$. The energy spectrum includes two branches with the linear dispersion

$$\epsilon_i^{\pm}=\pm\hbar v_{\perp}k_{\perp}+V, \tag{10}$$

while the wave function satisfies the differential equation

$$\left(\Delta(z)+\frac{\hbar^2k_{\perp}^2}{2m_{\perp}}-\frac{\hbar^2}{2m_{\parallel}}\frac{\partial^2}{\partial z^2}-\hbar v_{\parallel}\frac{\partial}{\partial z}\right)v^{\pm}=0. \tag{11}$$

To simplify the analytical calculation we consider a symmetry-inverted heterojunction, that is, the heterojunction in which $E_g(+\infty)=-E_g(-\infty)$. (This assumption is of no consequence on the final result, and generalization of this investigation for any heterojunction is trivial.) The gap function can be taken in the form

$$\Delta(z)=\Delta_0\tanh\left(\frac{z}{l}\right), \tag{12}$$

where $2\Delta_0=|E_g(+\infty)|=|E_g(-\infty)|$, and l defines the heterojunction width. We assume a gradual continuous transition between two layers, so as to avoid matching conditions at the interface which arise when a steplike transition region is considered. However, in doing so, it should be kept in mind that, in a graded heterojunction, in addition to the zero mode of the interface states there appear excited states.[12] The zero mode has been shown[7] not to depend on the transition region structure, and it was this state which has been studied in previous works.[4,5] We confine our attention to the zero mode.

Applying the following transformations to Eq. (11),

$$\xi=\tanh\left(\frac{z}{l}\right),$$

$$v(\xi)=(\xi+1)^p(\xi-1)^q\eta(x), \tag{13}$$

$$x=1/2(1-\xi),$$

where the parameters p and q are determined by the relations

$$q_{1,2}=-\frac{m_{\|}v_{\|}l}{2\hbar}\left\{1\pm\left[1+\frac{2}{m_{\|}v_{\|}^2}\left(\frac{\hbar^2k_{\perp}^2}{2m_{\perp}}+\Delta_0\right)\right]^{1/2}\right\},$$

$$p_{1,2}=-\frac{m_{\|}v_{\|}l}{2\hbar}\left\{-1\pm\left[1+\frac{2}{m_{\|}v_{\|}^2}\left(\frac{\hbar^2k_{\perp}^2}{2m_{\perp}}-\Delta_0\right)\right]^{1/2}\right\} \tag{14}$$

gives the hypergeometric equation

$$x(x-1)\eta''+[x(a+b+1)-c]\eta'+ab\,\eta=0, \tag{15}$$

where

$$a=p+q+1,$$

$$b=p+q,$$

$$c=2q+1+\frac{m_{\|}l}{\hbar}v_{\|}. \tag{16}$$

The index ''±'' was dropped here for simplicity. Thus we find that

$$\begin{aligned}v(\xi)=(\xi+1)^p(\xi-1)^q\{&C_1F[a,b,c;1/2(1-\xi)]\\&+C_2[1/2(1-\xi)]^{1-c}F[a-c+1,b-c+1,2\\&-c;1/2(1-\xi)]\}.\end{aligned} \tag{17}$$

The solution for the interface states being looked for here, the boundary conditions for them are $v\to 0$ when $\xi\to\pm 1$ (i.e. $z\to\pm\infty$). Solution (17) meets the boundary conditions when

$$C_2=0 \quad \text{and} \quad q>0, \quad 0<p<\frac{m_{\|}v_{\|}l}{\hbar},$$

and when

$$C_1=0 \quad \text{and} \quad q<-\frac{m_{\|}v_{\|}l}{\hbar}, \quad 0<p<\frac{m_{\|}v_{\|}l}{\hbar}.$$

The parameters p and q being real, only the zero mode of the interface states is of interest. Making use of Eq. (14), we find that interface states occur when

$$\Delta_0-\frac{m_{\|}v_{\|}^2}{2}<\frac{\hbar^2k_{\perp}^2}{2m_{\perp}}<\Delta_0. \tag{18}$$

Inequality (18) is the condition for interface states to appear, and shows that the far-band corrections result in cutting off the interface state energy spectrum both at large and small $k_{\perp}$. It is easy to show that the point $\hbar^2k_{\perp}^2/2m_{\perp}=\Delta_0$ is the intersection of one of the constituent bulk bands and the interface energy branch. Consequently, there is no interface state vanishing at $z\to\pm\infty$ when $\hbar^2k_{\perp}^2/2m_{\perp}>\Delta_0$. The identity $\hbar^2k_{\perp}^2/2m_{\perp}=\Delta_0$ has a deeper physical meaning. The value $\hbar^2k_{\perp}^2/2m_{\perp}$ at small $k_{\perp}$ can be considered as a half of the energy difference between two bulk branches of the initial semiconductors on both sides of the interface plane. Thus this is an energy uncertainty ΔE for our interface problem, which is related to the momentum uncertainty by $\Delta p=\Delta E/v_{\|}$. A coordinate uncertainty is determined by the de Broglie wavelength which, in the first approximation for the two-band Hamiltonian, is equal to $\lambda=\hbar/p=\hbar v_{\|}/\Delta_0$. Consequently, the uncertainty relation $\Delta p\Delta x\leqslant\hbar$ gives the following condition for the localized interface states:

$$\frac{\hbar^2k_{\perp}^2}{2m_{\perp}}\leqslant\Delta_0.$$

In the first approximation of the $\mathbf{k}\cdot\hat{\mathbf{p}}$ perturbation theory for the inverted symmetry heterocontact, by virtue of the energy spectrum symmetry, the energy uncertainty on the interface plane is equal to zero along all values of the transverse momentum. That is why there are no restrictions on the energy interval of the interface state existence.

The low limit in inequality (18) arises because there is no evanescent mode going to $z\to-\infty$ from the interface plane under the condition

$$\frac{\hbar^2k_{\perp}^2}{2m_{\perp}}<\Delta_0-\frac{m_{\|}v_{\|}^2}{2}$$

as $p_{1,2}$ become imaginary. This restriction, however, takes place just at $\Delta_0-m_{\|}v_{\|}^2/2>0$. For far-band masses as much as $m_{\|}v_{\|}^2/2\geqslant\Delta_0$, inequality (18) reduces to

$$0\leqslant\frac{\hbar^2k_{\perp}^2}{2m_{\perp}}\leqslant\Delta_0. \tag{19}$$

The disappearance of the interface mode at small $k_{\perp}$ can be understood in terms of another limiting case. When the semiconductor gap increases comparing to the energy difference between the actual extremes and the other remote bands, the single-band parabolic model of the electron energy spectrum is a good approximation. In the single-band limit the conduction and valence bands are completely decoupled and the Hamiltonian $\hat{H}_{00}$ [Eq. (1)] becomes diagonal. As a result the eigenvalue problem for the interface states reduces to the two independent equations.

$$\begin{aligned}&\left(\Delta(z)+\frac{\hbar^2k_{\perp}^2}{2m_{\perp}(z)}-\frac{\hbar^2}{2}\frac{\partial}{\partial z}\frac{1}{m_{\|}(z)}\frac{\partial}{\partial z}-\epsilon\right)\varphi(z)=0,\\&\left(-\Delta(z)-\frac{\hbar^2k_{\perp}^2}{2m_{\perp}(z)}+\frac{\hbar^2}{2}\frac{\partial}{\partial z}\frac{1}{m_{\|}(z)}\frac{\partial}{\partial z}-\epsilon\right)\chi(z)=0,\end{aligned} \tag{20}$$

with spatially varying masses $m_{\perp}$ and $m_{\|}$, which, in the parabolic approximation, are determined by

$$\begin{aligned}&\frac{1}{m_{\|,\perp}^A}=\frac{v_{\|,\perp}^2}{\Delta_0}\left(1+\frac{\Delta_0}{m_{\|,\perp}v_{\|,\perp}^2}\right) \quad \text{at } z>0,\\&\frac{1}{m_{\|,\perp}^B}=-\frac{v_{\|,\perp}^2}{\Delta_0}\left(1-\frac{\Delta_0}{m_{\|,\perp}v_{\|,\perp}^2}\right) \quad \text{at } z<0.\end{aligned} \tag{21}$$

Since the effective masses depend on $\Delta(z)$, a solution of Eqs. (20) with a smooth gap function like Eq. (12) is very complicated. However, by studying only the zero mode of the interface states we can confine ourselves to considering the steplike heterojunction determined by the conditions $\Delta(z)=\Delta_0$ at $z>0$ and $\Delta(z)=-\Delta_0$ at $z<0$. Interface states must be evanescent in nature. The envelope functions $\varphi(z)$ and $\chi(z)$ are localized at the interface, and decay exponen-

tially in both directions $\pm z$, submitting the Bastard boundary conditions which require that $\Psi(z)$ and $(1/m)[\partial\Psi(z)/\partial z]$ be continuous at the interface.[9] Such wave functions can meet the boundary conditions if only the effective mass $m_\parallel$ changes sign at the interface due to the band reversal, that is, at

$$m_\parallel^A m_\parallel^B < 0. \tag{22}$$

The interface energy spectrum is then

$$\epsilon_i^{\pm} = \pm\frac{\Delta_0^2}{m_\parallel v_\parallel^2} \pm \frac{\hbar^2 v_\perp^2 k_\perp^2}{2\Delta_0}\left(\frac{\Delta_0}{m_\perp v_\perp^2} + \frac{\Delta_0}{m_\parallel v_\parallel^2}\right). \tag{23}$$

As follows from Eq. (21), condition (22) means that $\Delta_0 < m_\parallel v_\parallel^2$. It is interesting to note that when $k_\perp = 0$ this solution tends to the result given in Ref. 13 where the interface states in the inverted HgTe-CdTe heterostructure were studied.

Comparing the two solutions obtained for the two-band and single-band models, we can draw the following conclusion. In spite of their difference as obvious results of two different approaches, both these solutions describe essentially the same interface states. The solution for the single-band model tends asymptotically to the one for the two-band model when $k_\perp = 0$ at $m_\parallel$, $m_\perp \to \infty$. The vanishing of the states when $\hbar^2 k_\perp^2/2m_\perp < \Delta_0 - m_\parallel v_\parallel^2/2$ in the two-band model is now related to their full disappearance in the single-band model at $\Delta_0 > m_\parallel v_\parallel^2/2$, when the effective masses of the initial semiconductors have the same sign. For the two-band model the interface state existence condition (18) is not so strong.

Finally, a trivial generalization of the above results for the case of nonsymmetrical heterocontact (both normal and inverted), but with still aligned constituent gap centers, is to define the gap function $\Delta(z)$ by

$$\Delta(z) = \Delta_+ + \Delta_- \tanh\left(\frac{z}{l}\right),$$

where $\Delta_\pm = (\Delta_A \pm \Delta_B)/2$, the parameters with index A or B being related to the initial semiconductors on the different sides from the interface boundary at $z>0$ or $z<0$, respectively. Then interface states with the linear spectrum along the transverse momentum (10) and with the wave function (17), by replacing $\hbar^2 k_\perp^2/2m_\perp \to (\hbar^2 k_\perp^2/2m_\perp) + \Delta_+$ and $\Delta_0 \to \Delta_-$, appear in the interval

$$-\Delta_B - \frac{m_\parallel v_\parallel^2}{2} \leqslant \frac{\hbar^2 k_\perp^2}{2m_\perp} \leqslant -\Delta_B. \tag{24}$$

Thus for a simple heterocontact with aligned constituent gap centers, a condition of the inverting band arrangement of one of the constituents (that is, $\Delta_B < 0$) is necessary but not sufficient, it also being necessary that the transverse momentum fall into the above allowed interval.

IV. STRESSED HETEROCONTACT WITH ANTIFERROMAGNETIC ORDERING

In this section we start from Eq. (5), assuming the parameters Δ, E, and V to be spatially varying functions and the antiferromagnetic ordering parameter L to be identical in both constituents. The coordinate dependence of all these functions may again be presumed to be described by a single function $f(z)$, such that $f(\pm\infty) = \pm 1$. From a physical point of view this assumption is reasonable. Moreover, since the zero mode of the interface states under consideration does not depend on the structure of the transition region, the form of the function $f(z)$ near the zero point is of no consequence in the final results. First of all a perturbative solution will be obtained.

A. Perturbative solution

By rotating the Hamiltonian in Eq. (5) we find

$$\tilde{\hat{H}} = \begin{pmatrix} V_+ + \tilde{\Delta}_+ \cos 2\theta - (W_\pm + E_+)\sin 2\theta & -Df(z) + \tilde{\Delta}_+ \sin 2\theta + (W_\pm + E_+)\cos 2\theta + ip_z \\ \text{H.c.} & V_+ + 2V_- f(z) - \tilde{\Delta}_+ \cos 2\theta + (W_\pm + E_+)\sin 2\theta \end{pmatrix}, \tag{25}$$

where $\tilde{\Delta}_+ = \Delta_+ + (\hbar^2 k_\perp^2/2m_\perp) - (\hbar^2/2m_\parallel)(\partial^2/\partial z^2)$, $D = \sqrt{\Delta_-^2 + E_-^2 - V_-^2}$, and the rotation angle is found from the equation

$$\Delta_- \cos 2\theta - E_- \sin 2\theta + V_- = 0.$$

Here the values of $E_\pm$ and $V_\pm$ are determined by the same relations as $\Delta_\pm$.

When the far-band corrections equal zero, so that $m_\parallel$, $m_\perp \to \infty$, one immediately obtains that the eigenvalue equation constructed on the Hamiltonian $\tilde{\hat{H}}$ has a solution with $\chi^\pm = 0$. This is the zero mode of the interface states discussed in Ref. 4. It has an energy spectrum

$$\epsilon_i^{\pm} = \Delta_+ \cos 2\theta - (W_\pm + E_+)\sin 2\theta + V_+. \tag{26}$$

The wave function is a solution of the differential equation

$$[-Df(z) + \Delta_+ \sin 2\theta + (W_\pm + E_+)\cos 2\theta + ip_z]\varphi^\pm(z) = 0.$$

These states are nondegenerate. Each of them is characterized by the average spin value[4]

$$\mathbf{S}_i^{\pm} = \varphi^\pm(z)\,\frac{2}{\tilde{L} \pm \sqrt{k_\perp^2 + \tilde{L}^2}}\,(k_y, -k_x, \tilde{L}),$$

being opposite directed along the z axis for the state φ^+ as compared to φ^-.

The normalization of these states results in cutting off their energy spectrum at a finite transverse momentum, so that the state φ^+ exists only inside the interval

$$-\frac{D}{|\cos 2\theta|}-\Delta_+\tan 2\theta-E_+<\hbar v_\perp\sqrt{k_\perp^2+\tilde{L}^2}<\frac{D}{|\cos 2\theta|}-\Delta_+\tan 2\theta-E_+, \tag{27}$$

while the state φ^- exists inside the interval

$$-\frac{D}{|\cos 2\theta|}+\Delta_+\tan 2\theta+E_+<\hbar v_\perp\sqrt{k_\perp^2+\tilde{L}^2}<\frac{D}{|\cos 2\theta|}+\Delta_+\tan 2\theta+E_+. \tag{28}$$

The positive definiteness of $\sqrt{k_\perp^2+\tilde{L}^2}$ means, that, if the left sides of these inequalities are less than zero, then they should be replaced by zero. Moreover, the states φ^+ or φ^- appear just in the event that the right sides of inequalities (27) and (28) are greater than L.

It is worth noting that these inequalities have a simple interpretation. Their limit points determine the intersections between one of the interface branches and the corresponding bulk band with the same spin direction. It is easy to show that inequalities (27) and (28) admit limiting transitions to particular cases discussed in Refs. 6 and 4. For example, in the case of the symmetry-unstressed inverted contact under the conditions $V_\pm=0$, $E_\pm=0$ and $\Delta_+=0$, we have $\cos 2\theta=0$, and so there is no cutoff of the states $\varphi^\pm$ in the transverse momentum region. In the case of the symmetry-stressed heterocontact at $\Delta_+=0$ and $E_+=0$, both states are cut off at just the same values of the transverse momentum as shown in the previous work.[4] Inequalities (27) and (28) also show that in non-symmetry-stressed heterocontact at $\Delta_+\neq 0$ or/and $E_+\neq 0$, the allowed interface intervals for the states φ^+ and φ^- are rather different. Then it follows that, in the case $\Delta_-^2>V_-^2$, giving a finite overlap of the gaps in the two constituents, the states φ^+ and φ^- both appear when $\Delta_A\Delta_B<0$ (i.e., the inverted contact). But in the case of the normal contact, when $\Delta_A\Delta_B>0$, only one of states φ^+ or φ^- is allowed by these conditions.

We may turn now to the full eigenvalue Schrödinger equation (25), taking into account all the far-band corrections. A solution with $\chi_\pm=0$ is not available now. However, as a first approximation in Eq. (25), one can neglect $\partial^2\varphi/\partial z^2$ compared to $\partial\varphi/\partial z$. Then one obtains the formal solution Eq. (26) by replacing $\Delta_+\rightarrow\Delta_+(\hbar^2k_\perp^2/2m_\perp)$. The allowed transverse momentum interval is again described by the inequalities like Eqs. (27) and (28) with the above replacement. This approximation is reliable under the condition

$$\frac{\hbar}{2m_\parallel v_\parallel}\left|\frac{\frac{\partial^2\varphi}{\partial z^2}}{\frac{\partial\varphi}{\partial z}}\right|\leqslant 1. \tag{29}$$

TABLE I. Model parameters of the bulk semiconductors.

	E_g (eV)	$2m_0v_\perp^2$ (eV)	$v_\perp/v_\parallel$	$m_\parallel v_\parallel^2$ (eV)	$m_\perp v_\perp^2$ (eV)
PbTe	0.189	6.02	3.4	0.169	0.229
PbSe	0.146	3.6	1.35	0.526	0.505

Finally, after simple calculations we find that there is a real region in the allowed transverse momentum interval determined by inequalities (27) and (28), where condition (31) proves to be fulfilled. After comparing with the numerical calculations, this trivial and simple approximation will be shown to describe a real interface spectrum quite well.

B. Numerical solution

Starting again from the Schrödinger equation (5), we are looking for an interface solution in the form of the exponentially decaying functions. For a step heterojunction with a sharp change of all the band parameters at the interface, the boundary conditions need to be applied to the eigenvalue problem to match the wave functions and their derivatives at the interface boundary. The appropriate conditions are found from the traditional treatment of the step heterojunction.[14] Assuming the wave function to be continuous at the interface and integrating the Schrödinger equation (5) across the interface boundary, we find the boundary conditions to be reduced to

$$\begin{aligned}&\varphi^\pm(z)|_{-0}=\varphi^\pm(z)|_{+0},\quad \varphi^{\pm\prime}(z)|_{-0}=\varphi^{\pm\prime}(z)|_{+0},\\ &\chi^\pm(z)|_{-0}=\chi^\pm(z)|_{+0},\quad \chi^{\pm\prime}(z)|_{-0}=\chi^{\pm\prime}(z)|_{+0}.\end{aligned} \tag{30}$$

Here the multiplies $1/m_\parallel^A$ and $1/m_\parallel^B$ in the boundary conditions for the derivatives of the wave functions are canceled due to our assumption that $m_\parallel^A=m_\parallel^B$.

After solving the boundary-value problem for the set of the second-order differential equations, one can write the dispersion relation for the interface states. A numerical solution of this transcendental equation results in the energy spectrum of the interface states, since then the wave functions are found.

To define this numerical calculation completely, the values of the model parameters now have to be determined. The problem of a general description of the energy spectrum is beyond this work. Instead we choose, as model band parameters, values characteristic of the semiconductors PbTe and PbSe. In doing so, we take into account that far-band corrections for semimagnetic semiconductors with a small content of magnetic ions can be assumed[15] to be identical to those in nonmagnetic host materials. The band parameters, including the far-band masses, are taken from Ref. 15, and are given in Table I. However, since the mirror symmetry band model is used, the far-band corrections are taken as an average between the values for the conduction and valence bands. Making use of the estimations obtained in Ref. 4, we give the parameter E, determining the stressed induced polarization effect, a value between 10 and 100 meV. The parameter L, describing the antiferromagnetic ordering, is taken equal to 20 meV for any semiconductor heterojunctions showing antiferromagnetic ordering.

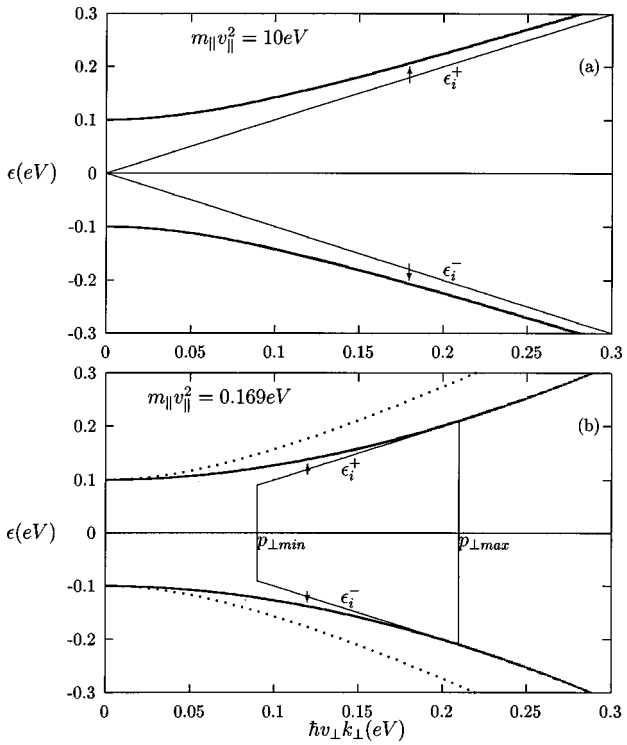

FIG. 1. Interface energy spectrum (thin lines) and energy branches of the constituents (dotted lines for semiconductor A and bold lines for semiconductor B) in the symmetry-inverted heterocontact without far-band corrections (a) and with them (b). The arrows show the spin direction for the interface states.

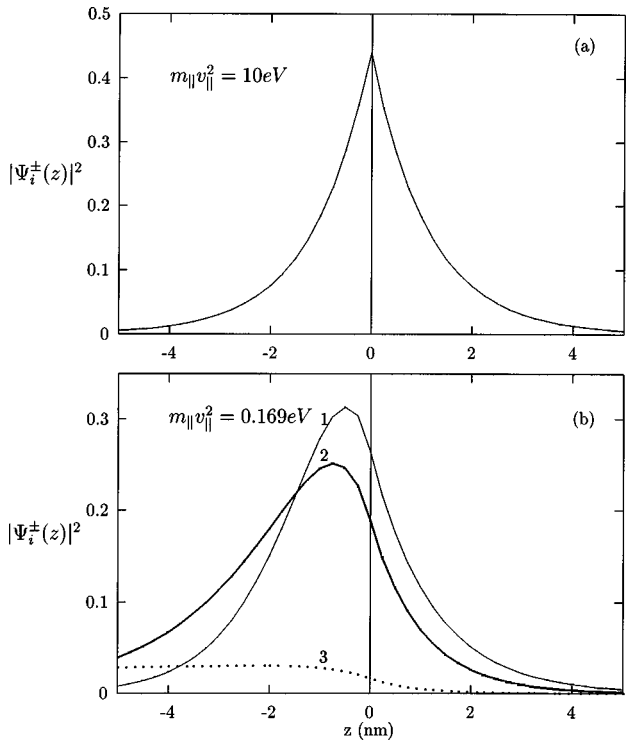

FIG. 2. Probability density function for the interface states of the symmetry-inverted heterocontact without far-band corrections (a) and with them (b) at $\hbar v_\perp k_\perp = 0.09$ eV (1), 0.015 eV (2), and 0.22 eV (3).

We first consider the simplest symmetry-inverted heterocontact. It is supposed that $\Delta_A = -\Delta_B$, $E_A = E_B = 0$, $L = 0$, and $V_A = V_B = 0$. Figure 1 shows the interface energy spectrum (thin lines) and the energy bands of the constituents (bold lines), without far-band corrections in Fig. 1(a) and with them in Fig. 1(b). Band parameters characteristic of PbTe (Table I) are used. If far-band terms are not included [Fig. 1(a)], the constituent bulk bands on both sides of the interface boundary go in the same way without intersecting the interface branches, coinciding perfectly with the theoretical curve [Eq. (10)].

Far-band corrections are included in Fig. 1(b). When $k_\perp$ increases the constituent bulk bands part, the conduction band of the semiconductor on the left side ($z<0$, $E_{gB}<0$) going down, while the one on the right side ($z>0$, $E_{gA}>0$) going up. This effect is stronger for small far-band masses, causing, in the end when $\hbar^2 k_{\perp\max}^2/2m_\perp = \Delta_0$, an intersection between the bulk conduction $\epsilon_\pm^{c,B}$ or valence $\epsilon_\pm^{v,B}$ bands and the corresponding interface branches $\epsilon_i^\pm$. Figure 1(b) also shows that the interface states disappear at $|k_\perp| < k_{\perp\min}$. This is in full agreement with the analytical solution for the simple heterocontact. The disappearance of the interface states was shown to be related to the peculiarities of the constituent band structures when $\Delta_0 > m_\parallel v_\parallel^2$. It is worth noting that for a symmetry-inverted heterocontact with parameters characteristic of PbSe, the interface energy branches exist in the whole interval $0 < \hbar^2 k_\perp^2/2m_\perp < \Delta_0$ without disappearing near the point $k_\perp \sim 0$, because $\Delta_0 < m_\parallel v_\parallel^2$ (see Table I).

The localization properties of the interface states under discussion are examined with the help of the probability density function, that is, the square of the envelope wave function of the interface states normalized on the whole volume of the structure versus the coordinate z, which is shown in Fig. 2 for the above two cases. The interface wave function for the heterojunction without far-band corrections [Fig. 2(a)] is quite symmetrical, being strongly localized near the interface. Its form depends weakly on $k_\perp$, the decay length being determined by the value of $\Delta_- /\hbar v_\parallel$ in agreement with the analytical results.

When far-band corrections are included, the probability density function takes the form shown in Fig. 2(b) at the beginning, middle, and end points of the allowed transverse momentum interval (lines 1, 2, and 3 in the Fig. 2, respectively). The form of the function $|\Psi_i^\pm(z)|^2$ depends strongly on $k_\perp$, being asymmetrical relative to the interface plane. Approaching the limit value $k_{\perp\max}$, the interface state energy goes up to the bulk bands $\epsilon_\pm^{c,B}$ and $\epsilon_\pm^{v,B}$, leading to a greater smearing of the functions $|\Psi_i^\pm(z)|^2$ [line 3 in Fig. 2(b)] on the side of the semiconductor referred to as $B(z<0)$, while their amplitudes do not change greatly. It is interesting to note that, at the limiting point $k_{\perp\max}$, the energy uncertainty $\Delta E_i^\pm$ of the interface mode, determined by the decay length, becomes comparable with the energy difference between two corresponding bulk bands $\Delta E_\pm^c = |\epsilon_\pm^{c,A} - \epsilon_\pm^{c,B}|$ or $\Delta E_\pm^v = |\epsilon_\pm^{v,A} - \epsilon_\pm^{v,B}|$ on the different sides of the interface boundary. As discussed in Sec. III, localized states meet the uncertainty principle just under the condition $\Delta E_i^\pm < \Delta E_\pm^{c,v}$, which is fulfilled inside the allowed interface interval, while it is broken at the limit points.

These results provide a good background for studying the

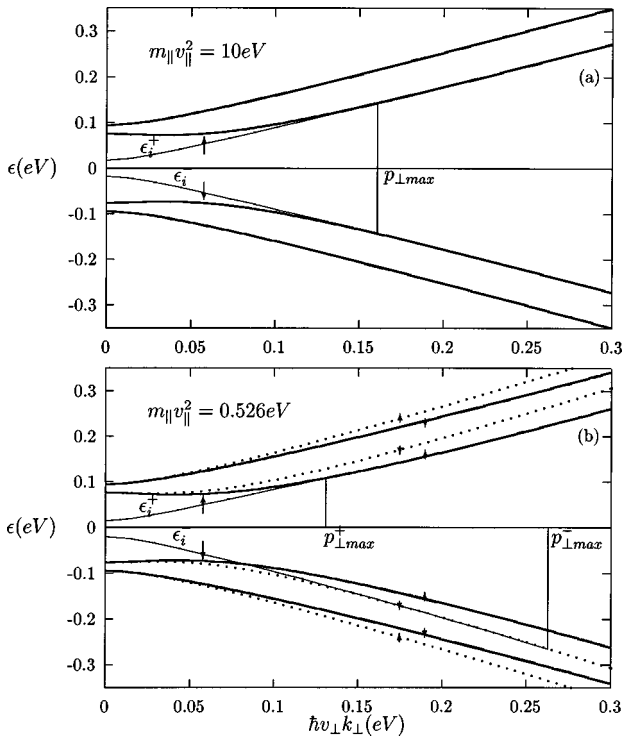

FIG. 3. Interface energy spectrum (thin lines) and energy branches of the constituents (dotted lines for semiconductor A and bold lines for semiconductor B) in the stressed symmetry-inverted heterocontact with antiferromagnetic ordering without far-band corrections (a) and with them (b). The arrows show the average spin direction.

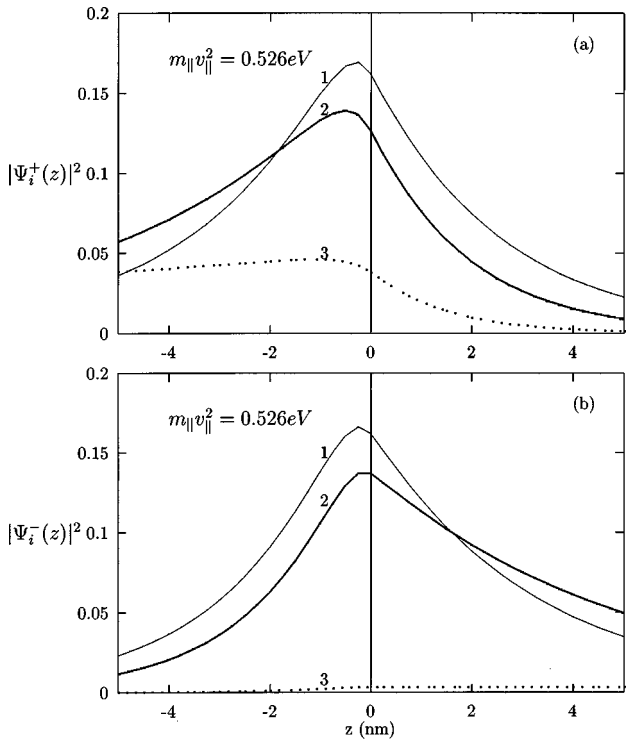

FIG. 4. Interface probability density function corresponding to the case shown in Fig. 3(b) for the state with spin up (a) at $\hbar v_\perp k_\perp = 0$ (1), 0.07 eV (2), and 0.13 eV (3) and for the state with spin down (b) at $\hbar v_\perp k_\perp = 0$ (1), 0.07 eV (2), and 0.26 eV (3).

interface energy spectrum of stressed heterojunctions based on semimagnetic semiconductors with antiferromagnetic ordering along the structure axis. In contrast to the simple heterojunction, all the constituent bulk bands are now spin split [see Eq. (7)], the bands $\epsilon_+^{c,v}$ and $\epsilon_-^{c,v}$ being characterized by opposite spin directions [Eq. (8)]. Being generated by bulk bands and, moreover, by bands with corresponding spin directions, the interface states ϵ_i^+ or ϵ_i^- with spin-up or spin-down relative to the z axis are bound up with all changes in the corresponding bulk energy spectrum caused by far-band corrections.

At first the stressed symmetry-inverted heterocontact with antiferromagnetic ordering is considered (Fig. 3). Band parameters characteristic of PbSe (see Table I) are now used. The other model parameters are taken as $\Delta_A = -\Delta_B$, $E_A = -E_B = 0.04$ eV, $L = 0.02$ eV, and $V_A = V_B = 0$. Figure 3(a) shows the energy bands for this heterocontact when far-band corrections are neglected. The interface spectrum consists of two branches ϵ_i^+ and ϵ_i^-, which exist just inside the restricted transverse momentum interval in full agreement with conditions (27) and (28). It is worth emphasizing that it is this heterocontact which was analytically considered in Ref. 4. Full coincidence between the analytical and numerical results makes us sure of the correctness of the numerical calculations.

Far-band corrections are included in Fig. 3(b). Constituent bulk bands with spin-up and -down do not change in the same way as before. Instead, there is an increase of the allowed momentum interval for the state ϵ_i^- and a decrease of the one for the state ϵ_i^+. We will see that this is the case when the interface magnetization effect is manifested more strongly after including far-band corrections, because even for fully completed interface bands the magnetization of one interface band is not compensated by the others with the opposite spin direction.

The interface probability density function for the case in Fig. 3(b) is shown in Fig. 4, again at the beginning, middle, and end points of the allowed transverse momentum interval (lines 1, 2, and 3 in the Fig. 4, respectively). Near the point $k_\perp \sim 0$ (line 1) the wave function for both states with spin-up and -down is nearly symmetrical. When the transverse momentum $k_\perp$ approaches the limit points in line 3 (which are different for the states ϵ_i^+ and ϵ_i^-), the interface state ϵ_i^+ (ϵ_i^-) goes up to the conduction bulk band $\epsilon_+^{c,B}$ (down to the valence band $\epsilon_-^{v,A}$), smearing at a greater distance on the side of the semiconductor B, that is, at $z<0$ [Fig. 4(a)] (on the side of semiconductor A at $z>0$ [Fig. 4(b)]).

Figure 5 gives an example of a normal stressed heterojunction with aligned constituent gap centers and showing antiferromagnetic ordering, which is determined by the parameters $\Delta_A = 0.1$ eV, $\Delta_B = 0.02$ eV, $E_A = 0.04$ eV, $E_B = 0.008$ eV, $L = 0.02$ eV, and $V_A = V_B = 0$. Far-band parameters characteristic of PbSe (Table I) are used. In this case only the interface state ϵ_i^- exists in full agreement with inequalities (27) and (28). The interface states of the normal heterocontact was shown[4] to appear inside either the conduction or valence bands of the constituents. In Fig. 5 one can see the interface energy branch with the determined spin direction touching the bulk bands of both constituents with the same spin direction in the limit points of the allowed mo-

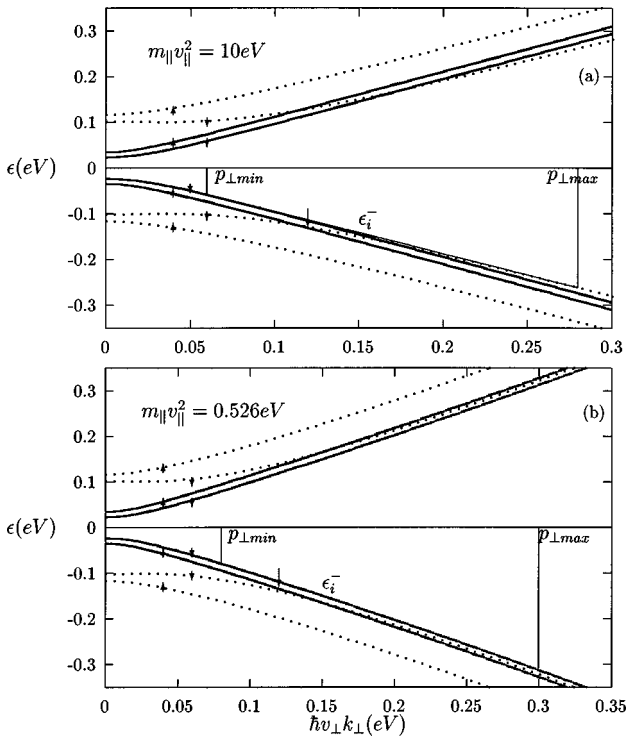

FIG. 5. The same as in Fig. 3, but for the normal heterocontact.

mentum interval. It follows that a requirement on the intersection of the corresponding constituent bulk bands should be a necessary condition for appearing the interface states. There is a trivial justification for a possibility of finding the interface states in the normal heterocontact coming from the geometrical disposition of the constituent bulk bands.

The physical interpretation of this fact can be understood in the following way. The energy of any localized state should be negative with respect to the characteristic potentials of the problem, the localization radius being determined by the decay length of the wave function, which is of the order of the de Broglie wavelength of the system.[16] When studying interface states of Tamm type, we begin with constituent bulk bands. Thus if there is a difference ΔU between the energies of the bulk bands (namely, the bands with the similar space and spin symmetry) on different sides of the interface boundary, then an interface state like $\exp(\pm\kappa z)$ (where κ is a decay length) has a chance of appearing only under the condition

$$\frac{\hbar^2\kappa^2}{2m_\parallel} > \Delta U. \tag{31}$$

This condition is certainly necessary but is not sufficient. Thus when two constituent bulk bands, intersecting in some point, part at the distance $\Delta U > \hbar^2\kappa^2/2m_\parallel$, the interface state generated by these bands disappears.

In the case including far-band corrections [Fig. 5(b)], the bulk bands of the constituents change quite differently, the energy spectrum of the semiconductor being more greatly affected by these corrections the greater the value of the gap. As a result, when decreasing the far-band masses (that means increasing the full far-band corrections), the valence bands $\epsilon_-^{v,A}$ and $\epsilon_-^{v,B}$ move toward each other, leading at first to an increase of the allowed momentum interval for the interface

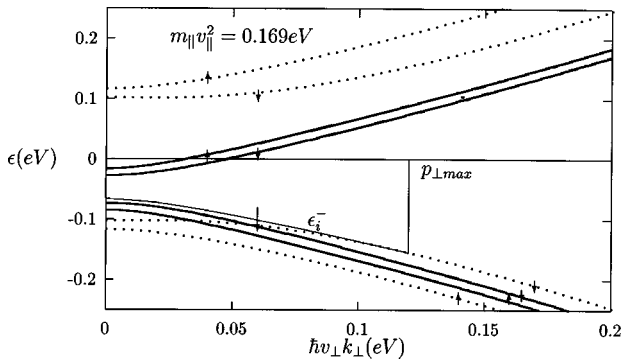

FIG. 6. The same as in Fig. 3, but for the nonsymmetry normal heterocontact. The case with far-band corrections is shown.

state existence. In the end, when the far-band masses approach the real values characteristic of PbSe (Table I), there is no intersection of these bands. However, Fig. 5(b) shows that an interface state still exists while condition (31) is fulfilled, just overlapping with the band $\epsilon_-^{v,B}$. On increasing the far-band corrections even further (up to the values characteristic of PbTe), the bands $\epsilon_-^{v,A}$ and $\epsilon_-^{v,B}$ part at a greater distance. As a result the interface state disappears.

Thus the interface states are bound up with the constituent bulk bands, and their appearance or disappearance is affected by the model band parameters. The change of the parameter $V_B=0$ to $V_B=-0.05$ eV, meaning the change of the band offset, causes a displacement of the constituent bulk bands. As a result, in contrast to the case $V_A=V_B=0$, where there is no interface state at the far-band corrections characteristic of PbTe, there appears an interface state ϵ_i^- shown in Fig. 6.

A structure, in which the gap parameter $\Delta(z)$ depends on the coordinate z in the opposite way to the polarization potential $E(z)$, is now considered. The following model parameters are used: $\Delta_A=0.1$ eV, $\Delta_B=0.01$ eV, $E_A=0.008$ eV, $E_B=0.04$ eV, $L=0.02$ eV, $V_A=0$, and $V_B=0.05$ eV. We note that the only difference in this heterojunction from the above example is the interchanges $E_A \leftrightarrow E_B$ and $V_B \rightarrow -V_B$. This is reasonable, and implies that the constituent with the smaller gap is affected by the polarization field more than the one with the greater gap. Figure 7 shows that there are interface branches with both spin-up and -down in this case. Since these branches are located near small-$k_\perp$

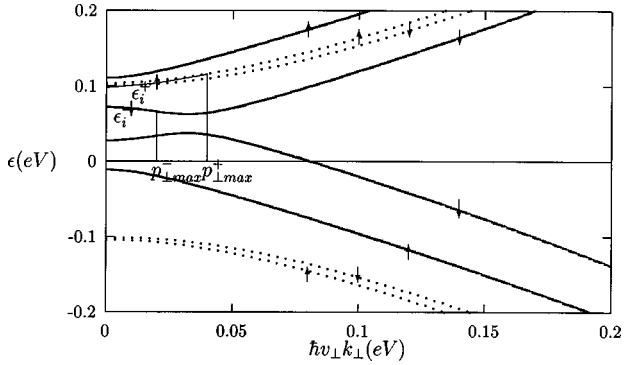

FIG. 7. The same as in Fig. 3, but for the nonsymmetry normal heterocontact, in which the gap parameter $\Delta(z)$ depends on the coordinate z in the opposite way from the polarization potential $E(z)$.

values, far-band corrections are of little consequence for the energy spectrum. That is why the interface energy spectrum without far-band corrections is not shown here. This heterojunction is of interest because both interface branches appear in spite of being normal structure.

All these numerical calculations are in very good qualitative agreement with the perturbative analytical solutions. Moreover, the coincidence between the analytical and numerical results is so good that they are nearly shown as overlapping in the figures.

V. INTERFACE MAGNETIZATION EFFECT

The interface magnetization effect has been shown to be related to the spin polarization of the interface state along the antiferromagnetic vector of the heterostructure discussed. Being nondegenerate, each interface state of the stressed heterocontact with antiferromagnetic ordering can be characterized by an interface spin determined as an average value of the spin operator constructed on the full interface wave functions $\Psi_i^{\pm}(z)$ (Ref. 4),

$$\mathbf{S}_i^{\pm}(z)=(|\varphi_i^{\pm}(z)|^2+|\chi_i^{\pm}(z)|^2)\,\frac{2}{\tilde{L}\pm\sqrt{\tilde{L}^2+k_{\perp}^2}}\,(k_y,-k_x,\tilde{L}). \tag{32}$$

After integrating over the transverse momentum space, taking into account a normalization of the wave function, we can write the average spin as a vector along the z axis as

$$\langle \mathbf{S}_i^{\pm}(z)\rangle=\pm\frac{1}{(2\pi)^2}\,(0,0,\tilde{L})\int_{k_{\perp\min}}^{k_{\perp\max}} dk_{\perp}^2\,\frac{|\Psi_i^{\pm}(z)|^2}{\sqrt{\tilde{L}^2+k_{\perp}^2}}, \tag{33}$$

where $k_{\perp\min}$ and $k_{\perp\max}$ are the limiting points of the allowed transverse momentum interval, and $|\Psi_i^{\pm}(z)|^2=|\varphi_i^{\pm}(z)|^2+|\chi_i^{\pm}(z)|^2$. Thus the interface states ϵ_i^{+} and ϵ_i^{-} are characterized by the average spin values $\langle S_i^{\pm}\rangle$, oppositely directed along the z axis, being a function centered near the interface boundary and decaying in both directions $\pm z$, according to the spatially varying function $\Psi_i^{\pm}(z)$.

In order to estimate the value $\langle S_i^{\pm}\rangle$, the dependence of the functions $\Psi_i^{\pm}(z)$ on the transverse momentum $k_{\perp}$ should be taken into account. Since there is no analytical solution of the interface problem in the general case, one has to make use of numerical calculations for the interface wave function form. On the basis of this calculation, by putting the origin of the transverse momentum at the middle of the allowed interval, one can assume this function to be

$$|\Psi_i^{\pm}(z)|^2=\frac{v_{\parallel}^2\kappa_{\parallel}^3}{v_{\perp}^2(a^2+k_{\perp}^2)}, \tag{34}$$

where a is a function depending on z, being at a minimum near the point $z=0$ and going up at $z\to\infty$ in such way as to describe the coordinate dependence of the function $\Psi_i^{\pm}(z)$. After putting Eq. (34) into Eq. (33), the interface average spin can easily be obtained.

Now taking into account the Fermi-level location, we can draw conclusions about the interface magnetization effect. If the Fermi level lies in one of the interface bands so that its average spin is not compensated by the average spin of the other interface band, then the interface magnetization effect can be observed. In any single case, the interface magnetization is determined by the relation between the values $\langle \mathbf{S}_i^{+}\rangle$ and $\langle \mathbf{S}_i^{-}\rangle$, depending on the mutual displacement of the interface bands, and the Fermi level that, in its turn, depends on the material parameters.

It proved to be useful to calculate the so-called relative interface magnetization, i.e., the value of the interface magnetization relative to the magnetization determined by the bulk bands [see Eq. (8)]. After integrating $\langle S^{\pm}\rangle$ over the occupied states up to the Fermi level and assuming $\tilde{L}<a$, one obtains, at $z=0$,

$$M=\frac{\langle S_i^{\pm}(0)\rangle}{\langle S^{\pm}\rangle}\sim\frac{\hbar^3 v_{\parallel}^3\kappa_{\parallel}^3}{p_F v_{\parallel}}\,\frac{1}{\sqrt{(L^2+\hbar^2 v_{\perp}^2 k_{\perp\min}^2)(L^2+\hbar^2 v_{\perp}^2 k_{\perp\max}^2)}}. \tag{35}$$

Here $\hbar v_{\parallel}\kappa_{\parallel}$ can be considered as the average interface state energy, $\kappa_{\parallel}$ being a decay parameter. The value $p_F v_{\parallel}$ is certain to be the Fermi energy. Thus, in agreement with the previous result, the relation of the interface magnetization to the band magnetization is conditioned by the ratio between the energies of the occupied interface and band states. It is very important to note that the value of the antiferromagnetic parameter L is of little consequence for the relative interface magnetization. Moreover, this effect should be manifested for a rather small value of L. Now, if making use of parameters characteristic of the structures considered here (for example, $\hbar v_{\parallel}\sim 0.2$ eV nm, $\kappa_{\parallel}\sim 0.5$ nm^{-1}, $\epsilon_F\sim 0.1$ eV, $\hbar v_{\perp}k_{\perp\min}\sim 0$, and $\hbar v_{\perp}k_{\perp\max}\sim 0.1$ eV), we find the relative interface magnetization to be $M\sim 5$. This result proves the correctness of previous estimations[4] made neglecting far-band corrections. Therefore, we conclude that the interface magnetization may be a real effect for these structures. The effect of far-band corrections is not so simple, but it can be determined from the change of the bulk energy spectrum of the constituents.

VI. SUMMARY

Interface states bound to the interface boundary in stressed heterocontacts made of semimagnetic semiconductors both with normal and inverted band spectra, and showing antiferromagnetic ordering, have been investigated in detail. The two-band envelope-function approximation, which takes into account the twofold degeneracy of the conduction and valence bands explicitly, and far-band contributions in the second-order perturbative theory have been used as a model for Hamiltonian of these semiconductor structures. In this work we did not aim to describe the energy spectrum exactly (constructing a model Hamiltonian within some approximations discussed above), but sought the genesis of the interface effect and an understanding of its change under the influence of far-band corrections. Moreover, any correlation effects were beyond this consideration. This one-electron ap-

proximation can be supported by the specific physical properties of the semiconductor structures, resulting in a strong screening of the electromagnetic fields.[4,5] However, we keep in mind that, in the case of overlapping between interface and band constituent states, a self-consistent approach, treating the coupling effects, needs to be developed. This interesting problem will be studied in a subsequent publication.

Perturbative analytical consideration has been confirmed by numerical calculations, treating the solution of the boundary-value problem with the Bastard boundary conditions. Both the energy spectrum and the envelope wave function of the interface states have been obtained. When increasing far-band corrections from infinite far-band masses up to their real values, the change of the interface state spectrum has been studied.

The conclusions arrived at from these calculations are as follows. Being of Tamm type, the interface states are generated from the constituent bulk energy spectrum. Therefore, the effect of far-band corrections on them is bound up with the mutual movement of the bulk bands, resulting in an increase or decrease (in some cases even a full disappearance) of the allowed transverse momentum interval for the interface state existence. In the inverted heterocontact the interface branches with spin-up and spin-down do not change in the same way under far-band corrections. This can lead to an increasing interface magnetization in some special cases. As for the normal heterocontact, the conclusion drawn in Ref. 6 concerning the existence of only an interface branch is not adequate. If the polarization potential $E(z)$ and the gap parameter $\Delta(z)$ of the structure under consideration depend on the coordinate z in the same way (that is, for example, $\Delta_A > \Delta_B$ and $E_A > E_B$), then it is the only interface branch that appears. However, if the potentials $E(z)$ and $\Delta(z)$ depend on the coordinate z in the opposite way (that is, for example, $\Delta_A > \Delta_B$ but $E_A < E_B$), then there is the possibility of both interface branches appearing, being located inside the constituent gaps. Making use of characteristic estimates of the model parameters, one could find the value of the relative interface magnetization.

Experimental support for the interface magnetization can be found in the magnetic resonance investigation[17] of EuTe/PbTe antiferromagnetic superlattices, which show a specific behavior in the quasi-two-dimensional magnetic ordering, and in other magnetic effects[18] in the same superlattices. It is important to note that, in an application to nonmagnetic systems, the same Tamm-like states have been shown to play a crucial role in forming the energy spectrum of the interface two-dimensional states in HgTe/CdTe semiconductor heterostructures based on inverted semiconductors.[19]

All these results make us sure that the interface magnetization generated from the spin polarization of Tamm-type interface states may be a real effect in the structures considered. The author believes that this work will stimulate experimental investigations to deal with this interface problem, giving rise to great interest.

ACKNOWLEDGMENTS

The author wishes to thank M. Kriechbaum for putting forward the problem and for helpful discussions. The author is also grateful to Paul N. Butcher for criticism and for carefully reading the manuscript. It is a pleasure to thank the Condensed Matter Group of the Abdus Salam International Centre for Theoretical Physics for its kind hospitality during the final stages of this work.

*Electronic address: malkova@lises.as.md

[1] W. Grieshaber, A. Haury, J. Cibert, Y. Merl d'Aubigue, A. Wasiela, and J. A. Gaj, Phys. Rev. B **53**, 4891 (1996).
[2] S. V. Halilov, J. Henk, T. Scheunemann, and K. Feder, Surf. Sci. **343**, 148 (1995).
[3] S. V. Halilov, J. Henk, T. Scheunemann, and K. Feder, Phys. Rev. B **52**, 14 235 (1995).
[4] V. G. Kantser and N. M. Malkova, Phys. Rev. B **56**, 2004 (1997).
[5] N. M. Malkova and V. G. Kantser, J. Phys.: Condens. Matter **9**, 9909 (1997).
[6] V. G. Kantser and N. M. Malkova, Pis'ma Zh. Eksp. Teor. Fiz. **54**, 388 (1991) [JETP Lett. **54**, 384 (1991)].
[7] B. A. Volkov and O. A. Pankratov, Pis'ma Zh. Eksp. Teor. Fiz. **42**, 145 (1985) [JETP Lett. **42**, 178 (1985)].
[8] D. Agassi and V. Korenman, Phys. Rev. B **37**, 10 095 (1988).
[9] G. Bastard, Phys. Rev. B **24**, 5693 (1981); *Wave Mechanics Applied to Semiconductor Heterostructures* (Les Editions de Physique, Les Ulis, Cedex, FR, 1989), Vol. 91944.
[10] H. Pascher, P. Rothlein, M. Kriechbaum, N. Frank, and G. Bauer, Superlattices Microstruct. **8**, 69 (1990).
[11] D. L. Smith and C. Mailhiot, J. Appl. Phys. **63**, 2717 (1988).
[12] S. F. Dominguez-Adame, Phys. Lett. A **202**, 395 (1995).
[13] Y. R. Lin-Liu and L. J. Sham, Phys. Rev. B **32**, 5561 (1985).
[14] M. Kriechbaum, P. Kochevar, H. Pascher, and G. Bauer, IEEE J. Quantum Electron. **24**, 1727 (1988).
[15] G. Bauer, H. Pascher, and W. Zawadzki, Semicond. Sci. Technol. **7**, 703 (1992).
[16] F. J. Himpsel, Surf. Sci. **299/300**, 525 (1994).
[17] Z. Wilamowski, R. Buczko, W. Jantsch, M. Ludwig, and G. Sprigholz, Acta Phys. Pol. A **90**, 973 (1996).
[18] J. J. Chen, G. Dresselhaus, M. S. Dresselhaus, G. Springholz, C. Pichler, and G. Bauer, Phys. Rev. B **54**, 402 (1996).
[19] G. M. Minkov, A. V. Germanenko, V. A. Larionova, and O. E. Rut, Phys. Rev. B **54**, 1841 (1996).